Reactivity and Characterization of Transition-Metal Carbonyl Clusters Using UV Laser Desorption Mass Spectrometry

Glenn Critchley,[†] Paul J. Dyson,*[,‡] Brian F. G. Johnson,*[,§] J. Scott McIndoe[§] Rachel K. O'Reilly,[§] and Patrick R. R. Langridge-Smith*[,||]

Micromass UK Limited, Floats Road, Wythenshawe, Manchester, M23 9LZ, U.K., Department of Chemistry, The University of York, Heslington, York, YO10 5DD, U.K., Department of Chemistry, The University of Cambridge, Lensfield Road, Cambridge, CB2 1EW, U.K., and Department of Chemistry, The University of Edinburgh, West Mains Road, Edinburgh, EH9 3JJ, U.K.

Received February 5, 1999

The positive and negative ion ultraviolet laser desorption time-of-flight mass spectra of $[Ru_3(CO)_{12}]$ have been recorded, using a 337 nm N_2 laser, over a range of experimental conditions. In the negative ion spectra the parent ion is not observed, but peaks corresponding to the trinuclear cluster ions $[Ru_3(CO)_{11}]^-$, $[Ru_3(CO)_{10}]^-$, and $[Ru_3(CO)_9]^-$, derived directly from the parent by the successive loss of one to three CO groups, are present. In addition, peaks corresponding to cluster ions with nuclearities ranging from 2 to 11 are observed. The higher mass clusters in the negative ion spectra have considerably greater intensities than the trinuclear clusters, suggesting that stable higher nuclearity clusters have been generated during the laser desorption process. It would appear that, in general, these correspond to the series of carbonyl clusters derived from the thermal decomposition of $[Os_3(CO)_{12}]$ that have yet to be isolated for ruthenium. In the positive ion spectra peaks corresponding to $[Ru_3(CO)_{13}]^+$, $[Ru_3(CO)_{12}]^+$, $[Ru_3(CO)_{11}]^+$, and $[Ru_3(CO)_{10}]^+$ are observed. Other peaks corresponding to species containing from four to six ruthenium atoms are also present. In addition, the appearance of peaks corresponding to the dinuclear species $[Ru_2(CO)_8]^+$ and $[Ru_2(CO)_9]^+$ indicates that some fragmentation takes place. Representative mass spectra are shown and some mechanistic proposals are given concerning the possible ionization mechanisms and the effect these have on the clustering processes. Related phenomena have been observed in similar experiments on $[Fe_3(CO)_{12}]$ and $[Os_3(CO)_{12}]$, and their spectra are compared with those of $[Ru_3(CO)_{12}]$.

Introduction

The carbonyl cluster chemistry of both ruthenium and osmium has been developed extensively.[1] Surprisingly, despite their proximity in the periodic table, major differences have been seen. For example, whereas the thermal decomposition of $[Ru_3(CO)_{12}]$ leads almost exclusively to carbido species, such as $[Ru_6C(CO)_{17}]$,[2] the same reaction of $[Os_3(CO)_{12}]$ gives a comprehensive list of, among others, the higher nuclearity clusters $[Os_5(CO)_{16}]$, $[Os_6(CO)_{18}]$, $[Os_7(CO)_{21}]$, and $[Os_8(CO)_{23}]$.[3] Other members of the same series, e.g., $[Os_4(CO)_{14}]$, have been obtained by alternative means.[4] Overall, this gives rise to the sequence of carbonyls $[Os_3(CO)_{12}]$, $[Os_4(CO)_{14}]$, $[Os_5(CO)_{16}]$, and $[Os_6(CO)_{18}]$, which differ by an $Os(CO)_2$ capping unit and form a polytetrahedral growth series. The remaining clusters, $[Os_7(CO)_{21}]$ and $[Os_8(CO)_{23}]$, are members of a different series based on a central Os_6 unit, which form part of a sequence leading to the tetracapped octahedron found in the anionic cluster $[Os_{10}C(CO)_{24}]^{2-}$. There have been no reports of the corresponding series for ruthenium. The reasons for this difference in behavior are not clear but are almost certainly linked to a kinetic, rather than a thermodynamic, constraint. In this paper we report studies of the laser activation of $[Ru_3(CO)_{12}]$ which provide support for the existence of the related series of carbonyl clusters for ruthenium.

Transition-metal carbonyl complexes are known to undergo ion−molecule clustering in the gas phase. This phenomenon has been observed using electron impact ionization mass spectrometry[5] for simple complexes

* To whom correspondence should be addressed. B.F.G.J.: e-mail, bfgj1@cam.ac.uk; fax, +44 1223 336362. P.J.D.: e-mail, pjd14@york.ac.uk. P.R.R.L.-S.: e-mail, prrls@ed.ac.uk.

[†] Micromass UK Limited.

[‡] The University of York.

[§] The University of Cambridge.

[||] The University of Edinburgh.

(1) (a) Johnson, B. F. G.; Lewis, J. *Adv. Inorg. Chem. Radiochem.* **1981**, *24*, 225. (b) Abel, E. W.; Stone, F. G. A.; Wilkinson, G. *Comprehensive Organometallic Chemistry II*; Pergamon Press: Oxford, U.K., 1995; Vol. 7, Chapters 11−16. (c) Lewis, J.; Raithby, P. R. *J. Organomet. Chem.* **1995**, *500*, 227. (d) Dyson, P. J.; Johnson, B. F. G.; Martin, C. M. *Coord. Chem. Rev.* **1996**, *155*, 69. (e) Dyson, P. J. *Adv. Organomet. Chem.* **1998**, *43*, 43.

(2) Eady, C. R.; Johnson, B. F. G.; Lewis, J. *J. Chem. Soc., Dalton Trans.* **1975**, 2606.

(3) Nicholls, J. N.; Vargas, M. D. *Inorg. Synth.* **1989**, *26*, 295.

(4) Pomeroy, R. K. *J. Organomet. Chem.* **1990**, *383*, 387.

(5) We thank a referee for drawing our attention to this work.

10.1021/om990075f CCC: $15.00
Publication on Web 09/08/1999

such as $Ni(CO)_4$,[6] $Fe(CO)_5$,[7] $Co(NO)(CO)_3$,[8] and $Cr(CO)_6$.[9] The development of FTICR mass spectrometry[10] enabled much more detailed studies of such gas-phase reactions, due to the very high mass resolution of the technique and the ability to extend the time scale of the experiment. Clusters have been examined using EI-FTICR, with cluster cations as large as $[Mn_8(CO)_{25}]^+$ formed from $Mn_2(CO)_{10}$ and $[Re_3Mn_3(CO)_{19}]^+$ from $ReMn(CO)_{10}$.[11] In similar experiments on $Os_3H_2(CO)_{10}$, self-reaction via gas-phase ion−molecule reactions has been found to produce clusters containing up to 15 osmium atoms upon extended (≥0.5 s) trapping.[12] Naked clusters can also be generated by progressive stripping of the carbonyl ligands. ^{252}Cf plasma desorption has also been shown to result in aggregation of clusters.[13]

The use of laser desorption ionization time-of-flight mass spectrometry as a method for generating large cluster ions[14] is particularly attractive, as such instruments are increasingly available in many laboratories for studies using MALDI (matrix-assisted laser desorption ionization) and a wide range of precursor compounds can be used since they do not need to be volatile.[15] We report here on the UV laser desorption mass spectra of the trinuclear clusters $[M_3(CO)_{12}]$ (M = Fe, Ru, Os) using such an instrument. As well as recording spectra for these homoleptic species, we have also obtained LDI-TOF-MS data for $Os_3H_2(CO)_{10}$. As mentioned above, EI-FTICR mass spectra of $Os_3H_2(CO)_{10}$ have been reported previously, showing clustering up to 15 osmium atoms. We also observed clustering in our LDI-TOF mass spectra, although it did not extend to such high masses. The assignment of these clusters containing hydride ligands is more difficult, due to the lower mass resolution of our TOF mass spectra, and a comparison of these data with the earlier EI-FTICR mass spectra[12] will, therefore, be presented separately.

Results and Discussion

The UV laser desorption mass spectra of triruthenium dodecacarbonyl $[Ru_3(CO)_{12}]$ were recorded using a number of different UV laser desorption/ionization time-of-flight (TOF) instruments in both negative and positive mode under a range of conditions (see Experimental Section). The spectra vary slightly from instrument to instrument and as the operating conditions are changed. However, the following general features have emerged.

(i) Peaks corresponding to the intact parent cluster ion are not observed in negative ion mode: instead the highest observed Ru_3 peak corresponds to $[Ru_3(CO)_{11}]^-$. This is a relevant feature important to the following discussion.

(ii) Peaks are observed at higher masses than that of the Ru_3 precursor and are believed to arise from the formation of higher nuclearity clusters derived from $[Ru_3(CO)_{12}]$ by chemical rather than other means. These peaks are usually more intense than those of the parent for negative ions and less intense for the positive ions.

(iii) In positive ion mode peaks corresponding to clusters in which an additional CO ligand is attached to the parent are present; that is, for $[Ru_3(CO)_{12}]$ the observed ion is $[Ru_3(CO)_{13}]^+$.

(iv) Peaks arising from post source decay (dissociation of the cluster aggregates outside of the ion extraction region) are observed. This only takes place when the spectra are recorded in reflectron mode, and it has the effect of perturbing the centroid of the isotope envelopes for certain peaks.

To illustrate the above points in more detail, we have chosen representative negative and positive ion spectra of $[Ru_3(CO)_{12}]$, and they are shown in Figure 1. Clearly, they require careful analysis and interpretation, and this depends on an understanding of both the characteristic reactivity patterns of transition metal carbonyl clusters and the nature of their molecular structure, together with an appreciation of the laser desorption/ionization process.

Negative Ion Spectrum of $[Ru_3(CO)_{12}]$. The negative ion mass spectrum of $[Ru_3(CO)_{12}]$ is shown in Figure 1a over the range 300−1600 Da; peak centroids are listed in Table 1, together with their corresponding assignments. The first point to note is the absence of a parent ion, at ca. 639 Da, corresponding to the intact cluster, $[Ru_3(CO)_{12}]^-$. Peak centroids are observed at 612, 585, and 557 Da (viz., 28 mass units apart, the nominal mass of CO) and may be readily assigned to ions corresponding to the trinuclear clusters $[Ru_3(CO)_{11}]^-$, $[Ru_3(CO)_{10}]^-$, and $[Ru_3(CO)_9]^-$ derived directly from the parent via the stepwise loss of CO ligands. This feature is commonly encountered in many desorption/ionization techniques with these types of compounds. Figure 2a shows an expansion of the envelope of peaks centered at 612 Da together with the simulated spectrum for $[Ru_3(CO)_{11}]^-$. The observed peak fingerprint is essentially identical to the calculated spectrum and confirms the identity of the cluster ion.

The parent ion $[Ru_3(CO)_{12}]^-$ is not observed in the spectrum. One possible reason is that the ionization mechanism for $[Ru_3(CO)_{12}]$ involves dissociative electron attachment. This is to be expected since the neutral cluster $[Ru_3(CO)_{12}]$ is a saturated 48-electron system with all bonding MOs occupied and no low lying empty MOs are available for occupancy; as a consequence, it is not expected to undergo electron addition without CO ligand loss. During the laser desorption/ionization process a large amount of thermal energy is provided and this can also lead to carbonyl ligand loss to produce, for example, the unsaturated cluster $[Ru_3(CO)_{11}]$ with available empty orbitals that can then accommodate the

(6) Allison, J.; Ridge, D. P. *J. Am. Chem. Soc.* **1979**, *101*, 4998.
(7) (a) Foster, M. S.; Beauchamp, J. L. *J. Am. Chem. Soc.* **1971**, *93*, 4924. (b) Foster, M. S.; Beauchamp, J. L. *J. Am. Chem. Soc.* **1975**, *97*, 4808.
(8) Weddle, G. H.; Allison, J.; Ridge, D. P. *J. Am. Chem. Soc.* **1977**, *99*, 105.
(9) Kraihanzel, C. S.; Conville, J. J.; Sturm, J. E. *J. Chem. Soc., Chem. Commun.* **1971**, 159.
(10) Marshall, A. G. *Acc. Chem. Res.* **1985**, *18*, 316.
(11) Meckstroth, W. K.; Freas, R. B.; Reents, W. D., Jr.; Ridge, D. P. *Inorg. Chem.* **1985**, *24*, 3139.
(12) Mullen, S. L.; Marshall A. G. *J. Am. Chem. Soc.* **1988**, *110*, 1766.
(13) (a) Fackler, J. P., Jr.; McNeal, C. J.; Winpenny, R. E. P. *J. Am. Chem. Soc.* **1989**, *111*, 6434. (b) Feld, H.; Leute, A.; Rading, D.; Benninghoven, A.; Schmid, G. *J. Am. Chem. Soc.* **1990**, *112*, 8166. (c) McNeal, C. J.; Hughes, J. M.; Lewis, G. J.; Dahl, L. F. *J. Am. Chem. Soc.* **1991**, *113*, 372. (d) McNeal, C. J.; Winpenny, R. E. P.; Hughes, J. M.; Macfarlane, R. D.; Pignolet, L. H.; Nelson, L. T. J.; Irgens, T. G.; Vigh, G.; Fackler, J. P., Jr. *Inorg. Chem.* **1993**, *32*, 5582.
(14) (a) Dale, M. J.; Dyson, P. J.; Johnson, B. F. G.; Martin, C. M.; Langridge-Smith, P. R. R.; Zenobi, R. *J. Chem. Soc., Chem. Commun.* **1995**, 1689. (b) Dale, M. J.; Dyson, P. J.; Johnson, B. F. G.; Langridge-Smith, P. R. R.; Yates, H. T. *J. Chem. Soc., Dalton Trans.* **1996**, 771.
(15) Reichart, B. E.; Sheldrick, G. M. *Acta Crystallogr., Sect. B* **1977**, *33*, 173.

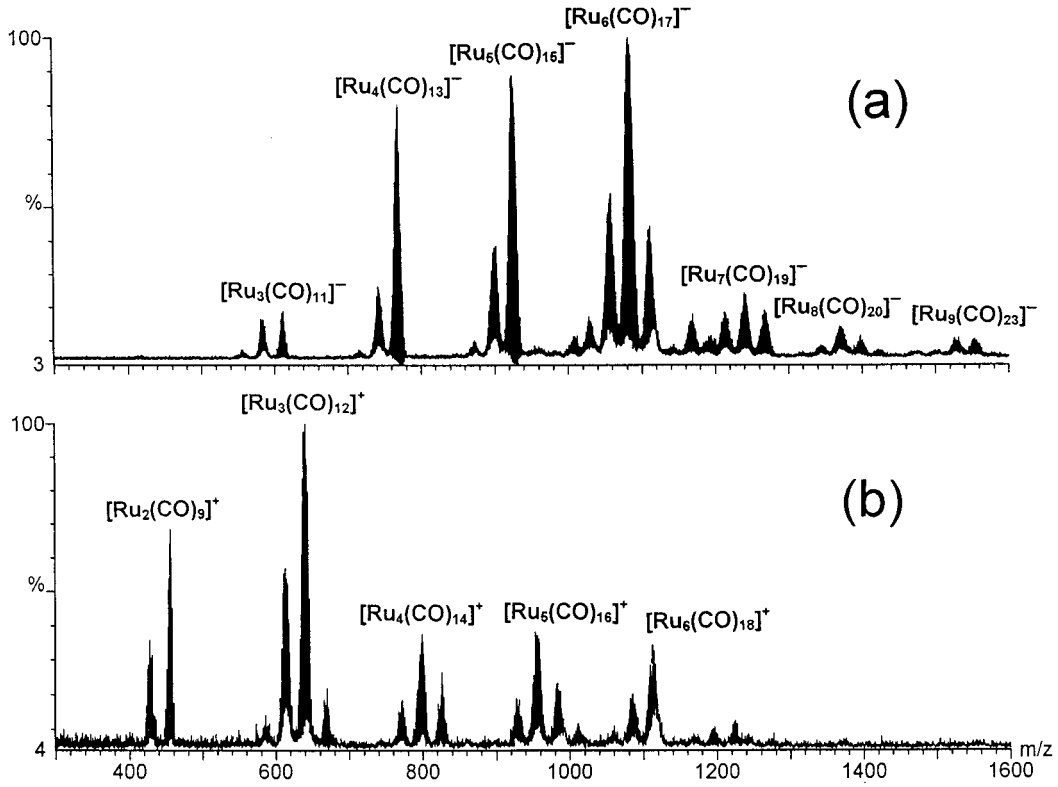

Figure 1. (a) Negative ion UV laser desorption mass spectrum of $Ru_3(CO)_{12}$, over the range 300−1600 Da, and (b) positive ion spectrum over the same mass range.

additional electron. It is worth noting that the first step in the dissociative electron attachment process might involve metal−metal bond cleavage.

Although the intact ion of $[Ru_3(CO)_{12}]$ is not observed in the spectrum, the mono-, bis-, and tris-decarbonylated species derived from the parent molecule are present. With this in mind, it is possible to postulate structures for the ions at masses above the trinuclear clusters observed in Figure 1, by the addition of a CO ligand to the highest mass peak for each cluster nuclearity. The cluster skeletal geometries inferred for the prominent ruthenium cluster ions seen in Figure 1 are listed in Table 1. These have been derived using the effective atomic number (EAN) rule, for clusters with nuclearities of four, five, and six, and the polyhedral skeletal electron pair theory (PSEPT) for clusters with six or more Ru atoms; see Table 2. In general, these are similar to those for the osmium carbonyl clusters that have been established in the laboratory (vide supra).

Three peaks with intensities greater than those assigned to the trinuclear clusters are observed at 769, 741, and 713 Da. These peaks may be assigned to the tetraruthenium cluster ions, $[Ru_4(CO)_{13}]^-$, $[Ru_4(CO)_{12}]^-$, and $[Ru_4(CO)_{11}]^-$, respectively (see Table 1). An expansion of the peak centered at 769 Da is shown in Figure 2b, together with a simulated spectrum for $[Ru_4(CO)_{13}]^-$, confirming the assignment. As in the case of the trinuclear species, the parent cluster is expected to have the formula $[Ru_4(CO)_{14}]$. According to the EAN rule, a cluster with this formula (i.e., 60 valence electrons) would have a tetrahedral core, as has been observed for the related osmium species. As mentioned above, such a cluster is unknown for ruthenium.

The next series of peaks is observed in the range 850−950 Da. The three peaks in this range, following arguments similar to those described above, may be assigned to cluster anions derived from the (suggested) parent cluster, $[Ru_5(CO)_{16}]$. The most intense peak envelope at 925 Da corresponds to the singly decarbonylated ion, $[Ru_5(CO)_{15}]^-$. Further CO loss results in the peaks centered at about 899 and 870 Da, which correspond to the cluster ions $[Ru_5(CO)_{14}]^-$ and $[Ru_5(CO)_{13}]^-$, respectively. Figure 2c shows an expanded view of the envelope of the peak centered at 925 Da, together with the simulated spectrum for $[Ru_5(CO)_{15}]^-$, which confirms this assignment. A cluster with formula $[Ru_5(CO)_{16}]$ is expected to have a trigonal bipyramidal arrangement of ruthenium atoms, and while such a cluster is not known for ruthenium, it has been observed for osmium.[15]

In the mass range 1000−1130 Da five main envelopes of peaks are observed. These may be assigned to fragments derived from the (hypothetical) octahedral parent $[Ru_6(CO)_{19}]$. As expected, a peak corresponding to this parent ion is not observed, but sequential decarbonylation gives rise to peaks centered at 1111, 1083, 1057, 1028, and 1000 Da, which are tentatively assigned to cluster ions of formula $[Ru_6(CO)_{17}]^-$, $[Ru_6(CO)_{16}]^-$, $[Ru_6(CO)_{15}]^-$, and $[Ru_6(CO)_{14}]^-$, respectively. The peak at 1111 Da corresponds to the monodecarbonylated species $[Ru_6(CO)_{18}]^-$, and is shown in Figure 2d together with the simulated spectrum. This peak shows some evidence of underlying post source decay (PSD, decay of the cluster ions in the flight tube).[16]

A series of lower intensity peaks due to PSD, centered at ca. 1118 Da and slightly staggered with respect to

(16) De Hoffmann, E.; Cherette, J.; Stroobant, V. *Mass Spectrometry*; John Wiley and Sons: Chichester, U.K., 1996.

Table 1: Peak Maxima for Principal Envelopes Seen in the Negative Ion UV Laser Desorption Mass Spectrum of $Ru_3(CO)_{12}$

peak centroid[a]	formula of ion	calculated mass	intensity (%)	possible polyhedron
1553.8	$[Ru_9(CO)_{23}]^-$	1555.0	7	tricapped octahedron
1525.8	$[Ru_9(CO)_{22}]^-$	1527.0	6	tricapped octahedron
1397.9	$[Ru_8(CO)_{21}]^-$	1397.1	6	bicapped octahedron
1369.9	$[Ru_8(CO)_{20}]^-$	1369.1	9	bicapped octahedron
1267.9	$[Ru_7(CO)_{20}]^-$	1268.2	15	monocapped octahedron
1240.0	$[Ru_7(CO)_{19}]^-$	1240.2	20	monocapped octahedron
1213.1	$[Ru_7(CO)_{18}]^-$	1212.2	13	monocapped octahedron
1197.1	$[Ru_6(CO)_{21}]^-$	1196.2	5	raft/doubly linked triangles
1169.2	$[Ru_6(CO)_{20}]^-$	1168.3	14	raft/trigonal prism
1111.1	$[Ru_6(CO)_{18}]^-$	1111.3	41	octahedron
1083.1	$[Ru_6(CO)_{17}]^-$	1083.3	100	bicapped tetrahedron
1057.2	$[Ru_6(CO)_{16}]^-$	1055.4	51	bicapped tetrahedron
1028.3	$[Ru_6(CO)_{15}]^-$	1027.4	12	bicapped tetrahedron
1000.4	$[Ru_6(CO)_{14}]^-$	999.4	6	bicapped tetrahedron
925.2	$[Ru_5(CO)_{15}]^-$	925.5	88	trigonal bipyramid
899.4	$[Ru_5(CO)_{14}]^-$	897.5	35	trigonal bipyramid
870.4	$[Ru_5(CO)_{13}]^-$	869.4	5	trigonal bipyramid
769.3	$[Ru_4(CO)_{13}]^-$	769.6	79	tetrahedron
741.5	$[Ru_4(CO)_{12}]^-$	741.6	23	tetrahedron
612.4	$[Ru_3(CO)_{11}]^-$	612.7	15	triangle
584.6	$[Ru_3(CO)_{10}]^-$	584.7	12	triangle
556.7	$[Ru_3(CO)_9]^-$	556.7	3	triangle

[a] Median measurements from single isotope resolved spectra; see Figure 2, for example. The difference between the measured and calculated peak centroids arises from the presence of post source decay fragments and is explained in the text.

the real peaks, prevents the baseline resolution observed in the other peaks shown in Figure 2. It is noteworthy that PSD is observed here and not for the smaller clusters, suggesting that the smaller clusters are more stable toward further decomposition in the flight tube. This could be due to the fact that the smaller clusters are *closo*-species and are therefore reluctant to undergo polyhedral modifications. With the larger, more open clusters, rearrangement of the metal core to a more compact configuration could occur and initiate the expulsion of CO. A pair of peaks centered at 1197 and 1169 Da do not appear to fit into the general pattern emerging from the growth sequence of *closo*- and capped *closo*-clusters described thus far. From a comparison of their isotopic distributions with simulated spectra these peaks are assigned to the hexaruthenium ions $[Ru_6(CO)_{21}]^-$ and $[Ru_6(CO)_{20}]^-$. For a ruthenium cluster with this number of carbonyl ligands the structure will need to be more open and the formula $[Ru_6(CO)_{21}]$ corresponds to the raft structure found for $[Os_6(CO)_{21}]$.[17] The fact that an electron is attached without loss of a carbonyl ligand is entirely reasonable given that the M_6 raft has a low lying empty MO susceptible to nucleophilic attack or even to two-electron reduction.[18] It is tempting to suggest, in the case of the Ru_6 species, that the raft $[Ru_6(CO)_{21}]$ is formed initially and that this undergoes systematic CO ejection to produce first the bi-edged bridged tetrahedron $[Ru_6(CO)_{20}]$, then the mono-edge bridged trigonal bipyramid $[Ru_6(CO)_{19}]$, and finally the tritetrahedron $[Ru_6(CO)_{18}]$, in a manner entirely established for the corresponding osmium derivative.[19] In which case ions may be produced both directly from a sequence of parents differing by one CO ligand and from a sequence of ions differing by one CO ligand. Alternatively, the formula $[Ru_6(CO)_{21}]$ might correspond to a trigonal prismatic structure, and the ion $[Ru_6(CO)_{21}]^-$ may have a structure in which a Ru−Ru bond of the trigonal prism has been cleaved.

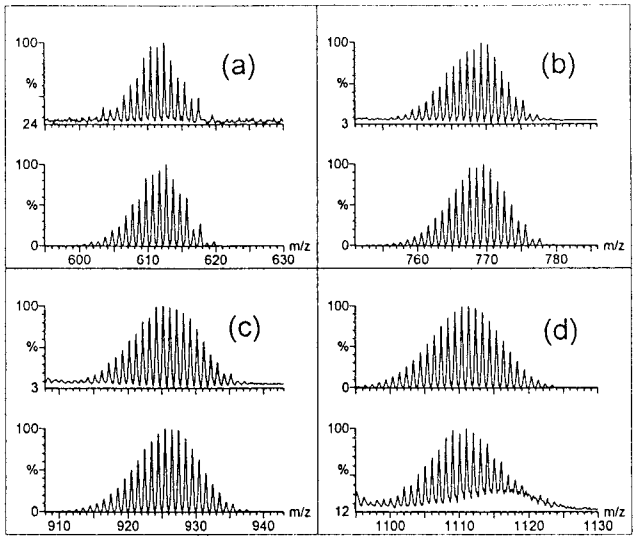

Figure 2. (a) Peak envelope centered at 612 Da from Figure 1a together with the simulated spectrum of $[Ru_3(CO)_{11}]^-$; (b) peak envelope centered at 769 Da together with the simulated spectrum of $[Ru_4(CO)_{13}]^-$; (c) peak envelope centered at 925 Da together with the simulated spectrum of $[Ru_5(CO)_{15}]^-$; (d) peak envelope centered at 1111 Da together with the simulated spectrum of $[Ru_6(CO)_{18}]^-$.

At masses beyond 1130 Da, additional peaks are observed with intensities similar in magnitude to those observed for the trinuclear cluster. The peaks centered at 1268, 1240, and 1213 Da may be readily assigned to the ions $[Ru_7(CO)_{20}]^-$, $[Ru_7(CO)_{19}]^-$, and $[Ru_7(CO)_{18}]^-$, corresponding to sequentially decarbonylated clusters derived from the (hypothetical) monocapped octahedral cluster $[Ru_7(CO)_{21}]$, which is similar to the known osmium derivative.[20] Low oxidation state transition-metal clusters of the iron triad do not tend to adopt *closo*-polyhedra beyond six metal atoms. Instead, they form condensed polyhedra in which the thermodynamically preferred polyhedron, the octahedron, is sequentially capped by $M(CO)_2$ units.

The peaks at 1397 and 1369 Da can be assigned to the octaruthenium ions of formula $[Ru_8(CO)_{21}]^-$ and $[Ru_8(CO)_{20}]^-$. These cluster ions may be derived from the hypothetical bicapped octahedral cluster $[Ru_8(CO)_{23}]$

(17) Farrar, D. H.; Johnson, B. F. G.; Lewis, J.; Nicholls, J. M.; Raithby, P. R.; Rosales, M. J. *J. Chem. Soc., Chem. Commun.* **1981**, 273.

(18) Evans, D. G.; Mingos, D. M. P. *Organometallics* **1983**, 435.

(19) Mason, R.; Thomas, K. M.; Mingos, D. M. P. *J. Am. Chem. Soc.* **1973**, *95*, 3802.

(20) Eady, C. R.; Johnson, B. F. G.; Lewis, J.; Mason, R.; Hitchcock, P. B.; Thomas, K. M. *J. Chem. Soc., Chem. Commun.* **1977**, 385.

Table 2: Comparison of Ruthenium Clusters Observed in the LDI-TOF Mass Spectrum of $Ru_3(CO)_{12}$ with Those Known for Osmium

tetrahedral growth sequence	*e* count	observed *closo*- and capped Os clusters	*e* count	observed negative ions
$[Ru_3(CO)_{12}]$	48	$[Os_3(CO)_{12}]^b$	48	$[Ru_3(CO)_{11}]^-$, $[Ru_3(CO)_{10}]^-$, $[Ru_3(CO)_9]^-$
$[Ru_4(CO)_{14}]$	60	$[Os_4(CO)_{14}]^b$	60	$[Ru_4(CO)_{13}]^-$, $[Ru_4(CO)_{12}]^-$
$[Ru_5(CO)_{16}]$	72	$[Os_5(CO)_{16}]^b$	72	$[Ru_5(CO)_{15}]^-$, $[Ru_5(CO)_{14}]^-$, $[Ru_5(CO)_{13}]^-$
$[Ru_6(CO)_{18}]$	84	$[Os_6(CO)_{18}]^b$	84	$[Ru_6(CO)_{20}]^-$, $[Ru_6(CO)_{19}]^-$, $[Ru_6(CO)_{18}]^-$, $[Ru_6(CO)_{17}]^-$, $[Ru_6(CO)_{16}]^-$, $[Ru_6(CO)_{15}]^-$, $[Ru_6(CO)_{14}]^-$
$[Ru_7(CO)_{20}]$	96	$[Os_7(CO)_{21}]^c$	98	$[Ru_7(CO)_{20}]^-$, $[Ru_7(CO)_{19}]^-$ *, $[Ru_7(CO)_{18}]^-$
$[Ru_8(CO)_{22}]$	108	$[Os_8(CO)_{23}]^c$	110	$[Ru_8(CO)_{21}]^-$, $[Ru_8(CO)_{20}]^-$ *
$[Ru_9(CO)_{24}]$	120			$[Ru_9(CO)_{23}]^-$, $[Ru_9(CO)_{22}]^-$
$[Ru_{10}(CO)_{26}]^a$	132			
$[Ru_{11}(CO)_{28}]$	144			$[Ru_{11}(CO)_{27}]^-$
$[Ru_{12}(CO)_{30}]^a$	156			

[a] Not observed. [b] Polyhedral growth sequence. [c] Sequence of capped octahedra.

by the loss of two CO groups. Support for this view comes from the known osmium analogue.[21] However, it is possible that these ions stem from the polytetrahedral species $[Ru_8(CO)_{22}]$, which has no known structural analogue.

The peaks at 1554 and 1526 Da correspond to the ions $[Ru_9(CO)_{23}]^-$ and $[Ru_9(CO)_{22}]^-$. Again these may be based on the next member of the series of capped octahedra, viz., $[Ru_9(CO)_{25}]$. However, in this case, as with the Ru_8 species, the parent may correspond to the polytetrahedral species $[Ru_9(CO)_{24}]$, with the highest intensity peak corresponding to the cluster ion $[Ru_9(CO)_{23}]^-$.

Under certain conditions, clustering beyond nine ruthenium atoms is observed, but the complex isotopic distributions, lower resolution at higher mass, and low intensities have so far precluded detailed assignment. However, one ion, which may be formulated as $[Ru_{11}(CO)_{27}]^-$, has been detected and assigned with confidence. Again, this may be derived either from the capped octahedral $[Ru_{11}(CO)_{29}]$ or the polytetrahedral cluster $[Ru_{11}(CO)_{28}]$. We have also conducted preliminary experiments using Fourier transform ion cyclotron resonance mass spectrometry (FTICR-MS) in conjunction with laser desorption ionization and have observed similar clustering behavior. The superior mass resolution that can be achieved using this technique will allow us to more fully characterize these high-nuclearity cluster ions. This work will be reported in due course.

Positive Ion Spectrum of $[Ru_3(CO)_{12}]$. The positive ion mass spectrum of $[Ru_3(CO)_{12}]$ is shown in Figure 1b. The peak centroids are listed in Table 3, together with their corresponding assignments and possible structures. The lowest mass species are observed at 455 and 427 Da and may be attributed to the dinuclear ions $[Ru_2(CO)_9]^+$ and $[Ru_2(CO)_8]^+$. The peak envelope for $[Ru_2(CO)_9]^+$ is shown in Figure 3a together with the simulated spectrum. These fragments presumably result from the ionization process and arise from the parent $[Ru_2(CO)_9]$, produced from the decomposition of $[Ru_3(CO)_{12}]$. The dinuclear complex, while highly reactive, can be prepared synthetically from $[Ru_3(CO)_{12}]$ by photolysis using matrix isolation techniques.[22]

Table 3: Peak Maxima for Principal Envelopes Seen in the Positive Ion UV Laser Desorption Mass Spectrum of $Ru_3(CO)_{12}$

peak centroid[a]	formula of ion	calculated mass	intensity (%)	possible polyhedron
1111.9	$[Ru_6(CO)_{18}]^+$	1111.3	35	bicapped tetrahedron
1084.0	$[Ru_6(CO)_{17}]^+$	1083.4	16	bicapped tetrahedron
1056.0	$[Ru_6(CO)_{16}]^+$	1055.4	5	bicapped tetrahedron
1009.8	$[Ru_5(CO)_{18}]^+$	1009.4	6	raft
982.0	$[Ru_5(CO)_{17}]^+$	981.4	20	square pyramid
954.0	$[Ru_5(CO)_{16}]^+$	953.4	39	trigonal bipyramid
926.2	$[Ru_5(CO)_{15}]^+$	925.5	15	trigonal bipyramid
826.1	$[Ru_4(CO)_{15}]^+$	825.5	24	butterfly
798.2	$[Ru_4(CO)_{14}]^+$	797.5	36	tetrahedron
770.3	$[Ru_4(CO)_{13}]^+$	769.6	14	tetrahedron
668.2	$[Ru_3(CO)_{13}]^+$	668.6	18	linear/bent
640.3	$[Ru_3(CO)_{12}]^+$	640.7	100	triangle
613.4	$[Ru_3(CO)_{11}]^+$	612.7	54	triangle
585.5	$[Ru_3(CO)_{10}]^+$	584.7	9	triangle
455.4	$[Ru_2(CO)_9]^+$	454.8	69	linear
427.4	$[Ru_2(CO)_8]^+$	426.8	35	linear

[a] Median measurements from single isotope resolved spectra; see Figure 2, for example. The difference between the measured and calculated peak centroids arises from the presence of post source decay fragments and is explained in some length in the text.

The most intense peak in the spectrum at 640 Da corresponds to the mass of the intact parent ion $[Ru_3(CO)_{12}]^+$. This peak envelope is shown in Figure 3b together with a simulated spectrum. A peak at 668 Da, ca. 28 Da above the parent, is also observed and is taken to correspond to $[Ru_3(CO)_{13}]^+$. In addition, peaks are also observed at 613 and 586 Da, which are typical of carbonyl loss from $[Ru_3(CO)_{12}]^+$, and correspond to the ions $[Ru_3(CO)_{11}]^+$ and $[Ru_3(CO)_{10}]^+$, respectively. Ionization is expected to cause an electron to be ejected from highest occupied MO of $[Ru_3(CO)_{12}]$ to produce $[Ru_3(CO)_{12}]^+$. Since $[Ru_3(CO)_{13}]^+$ is observed, it seems plausible that expulsion of an electron brings about the cleavage of a Ru−Ru bond and the coordinatively unsaturated cluster ion is able to add an additional CO ligand.

At higher masses, a series of less intense peaks are observed which extend to masses of ca. 1250 Da, somewhat less than that observed for the negative ions. In the range 750−830 Da, three peaks are observed and may be assigned to the tetraruthenium cluster ions $[Ru_4$-

(21) The structure of $[Os_8(CO)_{23}]$ has not been reported, but the structure of $[Os_8(CO)_{22}]^{2-}$ is known: Jackson, P. F.; Johnson, B. F. G.; Lewis, J.; Raithby, P. R. *J. Chem. Soc., Chem. Commun.* **1980**, 60.

(22) Moss, J. R.; Graham, W. A. G. *J. Chem. Soc., Dalton Trans.* **1977**, 95.

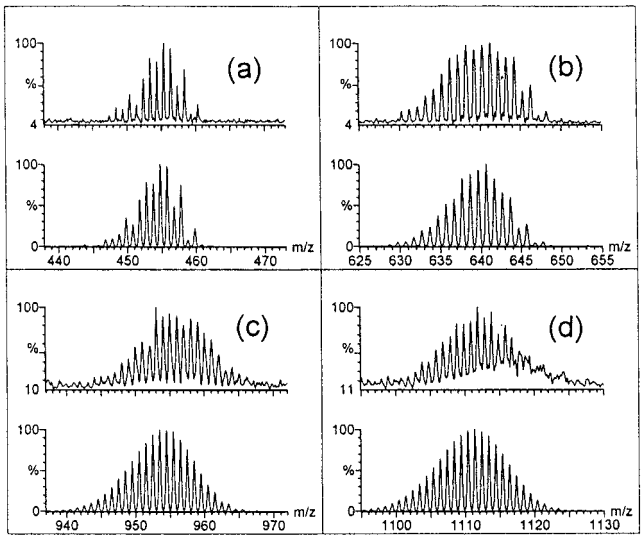

Figure 3. (a) Peak envelope centered at 455 Da from Figure 1b together with the simulated spectrum of $[Ru_2(CO)_9]^+$; (b) peak envelope centered at 640 Da together with the simulated spectrum of $[Ru_3(CO)_{12}]^+$; (c) peak envelope centered at 954 Da together with the simulated spectrum of $[Ru_5(CO)_{16}]^+$; (d) peak envelope centered at 1111 Da together with the simulated spectrum of $[Ru_6(CO)_{18}]^+$.

$(CO)_{15}]^+$, $[Ru_4(CO)_{14}]^+$, and $[Ru_4(CO)_{13}]^+$. An expansion of the peak centered at 826 Da is shown in Figure 3b, together with a simulated spectrum for $[Ru_4(CO)_{15}]^+$; their similarity confirms the assignment. Given the information from the negative ion spectrum, it is not unreasonable to suppose that these ions are derived from the tetrahedral parent $[Ru_4(CO)_{14}]$. On the basis of the assignments in the parent ion region, which involve CO addition and metal−metal bond cleavage, the highest mass peak, $[Ru_4(CO)_{15}]^+$, should correspond to a butterfly geometry derived from a tetrahedron in which one Ru−Ru bond has been cleaved. The osmium analogue is known.[4]

Peaks corresponding to pentanuclear clusters are observed between 900 and 1030 Da. The assignment of these peaks is straightforward, although the metal atom topology is less clear. This is because the number of possible structures for clusters with open geometries increases as the nuclearity increases, and as such, formulation becomes somewhat speculative. Peaks centered at 1010, 982, 954, and 926 Da can be assigned to the ions $[Ru_5(CO)_{18}]^+$, $[Ru_5(CO)_{17}]^+$, $[Ru_5(CO)_{16}]^+$, and $[Ru_5(CO)_{15}]^+$, respectively. It is possible that these ions are derived from the parent-raft cluster $[Ru_5(CO)_{19}]$, which is known for osmium.[23]

Peaks at 1112, 1084, and 1056 correspond to the hexaruthenium ions $[Ru_6(CO)_{18}]^+$, $[Ru_6(CO)_{17}]^+$, and $[Ru_6(CO)_{16}]^+$. These follow the expected general pattern of CO ejection from the stable neutral cluster $[Ru_6(CO)_{18}]$. While a cluster with this formula is unknown, the isoelectronic octahedral osmium cluster $[Os_6(CO)_{18}]^{2-}$ is known.[24] Since the metal−metal bonds in these larger clusters cannot be described in terms of 2c−2e bonds, the straightforward transformations that take place are much more complicated on loss of a two-electron CO ligand. For example, while the removal of two electrons from a tetranuclear group 8 butterfly cluster affords a tetrahedral cluster, a two-electron oxidation of the octahedral cluster $[Os_6(CO)_{18}]^{2-}$ affords the polytetrahedral cluster $[Os_6(CO)_{18}]$.[24]

Mechanistic Inferences. The generation of negative and positive ions has a profound influence on the nature of the cluster aggregates formed. Laser ablation of the sample produces a plasma containing neutrals and ions, both negative and positive; these have high internal energies and can reduce their energy in a number of ways including ionization, expulsion of carbonyl ligands, fragmentation, or condensation. In general, it is reasonable to suppose that the distribution of products is governed by kinetic rather than thermodynamic constraints. Nevertheless, it is possible to speculate on the observed product distribution. From previous observations of the corresponding thermal chemistry of $[Os_3(CO)_{12}]$, we have some idea of the expected nature and nuclearity of the derivatives. The mechanism by which they and the series of higher nuclearity osmium clusters are produced is difficult to establish. For osmium, a mechanism has been suggested but remains unsupported. This depends on the elimination of saturated fragments, such as $Os(CO)_5$, from cluster precursors, e.g., $[Os_3(CO)_{12}]$, and the combination of the remaining unsaturated fragments. It would seem that both the negative and positive ion mass spectra support this view of the initial process, since in each case ions produced apparently from the same precursor or parent are observed.

In the earlier EI−FTICR studies,[11,12] it was possible to investigate in detail the mechanism for "self-clustering" by examining the products from the ion−molecule reactions of selected precursor ions with the excess neutral parent present in the trapping cell. These reactions were followed over a time scale of several seconds. In contrast, in our experiments the desorption plume contains neutrals as well as anions and cations. Moreover, to enhance the mass resolution in our LDI-TOF mass spectra, they were all recorded using delayed ion extraction, in which the products formed following laser desorption remain in the ion source of the instrument for approximately 200 ns, before being pulse extracted into the reflecting geometry time-of-flight analyzer. Consequently, it is much more difficult to investigate the mechanism by which the supraclusters are formed, although ion−molecule or ion−ion chemistry must be dominant in view of the short time scale prior to product analysis.

Negative Ion Spectra for $Os_3(CO)_{12}$ and $Fe_3(CO)_{12}$. The negative ion mass spectrum of $Os_3(CO)_{12}$ is shown in Figure 4a over the range 0−2500 Da. The first series of peaks in the range 800−900 Da are attributable to the ions $[Os_3(CO)_x]^-$ (x = 9−11). As observed for the trinuclear Ru_3 clusters, no intact parent ion $[Os_3(CO)_{12}]^-$ is present. Instead, $[Os_3(CO)_{11}]^-$ is the highest mass trinuclear species observed. Progressive carbonyl losses from the metal core account for the remaining peaks in the series. The 950−1150 Da range contains tetranuclear clusters $[Os_4(CO)_x]^-$ (x = 10−13). The tetrahedral cluster $Os_4(CO)_{14}$ is a known species[4] and is likely to be the source of this series of clusters,

(23) Farrar, D. H.; Johnson, B. F. G.; Lewis, J.; Raithby, P. R.; Rosales, M. J. *J. Chem. Soc., Dalton Trans.* **1982**, 2051.
(24) Eady, C. R.; Johnson, B. F. G.; Lewis, J. *J. Chem. Soc., Chem. Commun.* **1976**, 302.

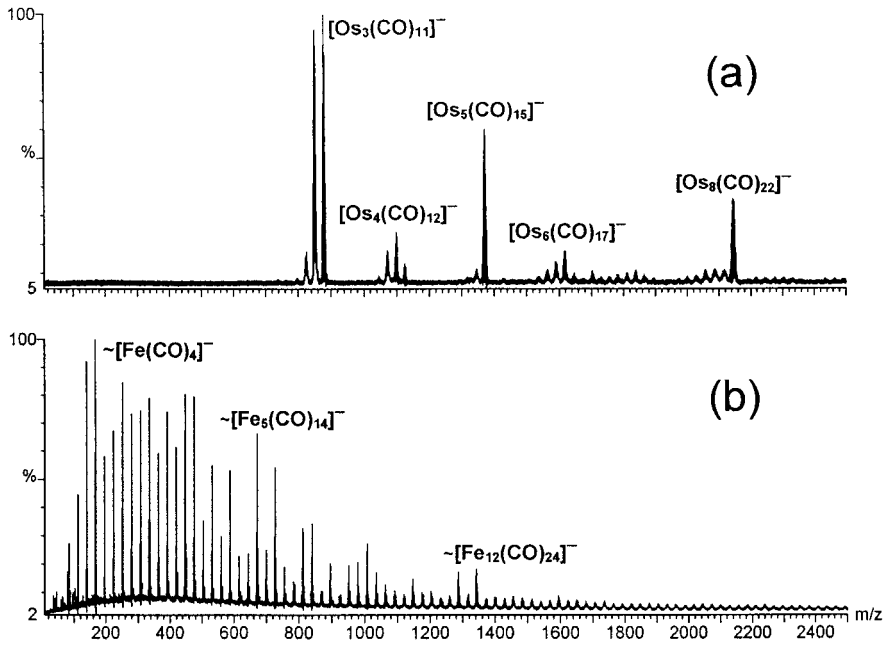

Figure 4. (a) Negative ion UV laser desorption mass spectra of $[Os_3(CO)_{12}]$, over the range 0−2500 Da, and (b) corresponding spectrum for $[Fe_3(CO)_{12}]$ over the same mass range.

as for the comparable tetrahedral ruthenium clusters. The peak at 1072 Da, corresponding to $[Os_4(CO)_{11}]^-$, is the most intense in the spectrum and contrasts with the M_6 clusters that dominate in the ruthenium spectrum. The next series of peaks is observed in the region 1300−1400 Da and may be assigned to the cluster anions formed by partial decarbonylation of $Os_5(CO)_{16}$, similar to that observed for ruthenium. This osmium cluster is known and has a trigonal bipyramidal structure.[15] Loss of CO from this cluster generates the observed ions $[Os_5(CO)_x]^-$ (x = 14−15). Between 1520 and 1630 Da a further set of peaks attributed to the cluster anions $[Os_6(CO)_x]^-$ (x = 14−17) are observed, presumably derived from the known cluster $Os_6(CO)_{18}$. Again, related peaks were observed in the ruthenium spectrum, although the peaks corresponding to the more open clusters, $[Ru_6(CO)_{21}]^-$ and $[Ru_6(CO)_{20}]^-$, were not observed here. Clearly, these tetra-, penta-, and hexanuclear clusters follow a polytetrahedral growth sequence that could also extend to the Os_7 and Os_8 clusters.

The range 1740−1870 Da contains a series of peaks of low intensity assigned to the heptanuclear cluster anions $[Os_7(CO)_x]^-$ (x = 15−19). The expected parent of this series would be either $Os_7(CO)_{20}$, an unknown cluster containing a polytetrahedral skeleton, or $Os_7(CO)_{21}$, a known cluster containing a capped octahedron of metal atoms. At the highest masses, 1970−2160 Da, a series of reasonably intense peaks readily assigned as $[Os_8(CO)_x]^-$ (x = 16−22) are seen. The expected structure of the parent cluster, $Os_8(CO)_{23}$, is that of a bicapped octahedron. Both of these sets of peaks were observed in the corresponding spectrum of $[Ru_3(CO)_{12}]$.

It has been found that increasing the laser power reduces the number of higher nuclearity species (Os_7, Os_8) produced and simultaneously increases carbonyl loss from each series of clusters. In addition, if the sample is dissolved in a matrix such as dithanol, less clustering is observed, but just as much fragmentation of each cluster to its decarbonylated daughter ions is seen. Decreased clustering is not unexpected, as laser ablation of the "diluted" sample would produce a lower concentration of neutrals and ions in the gas phase.

The negative ion spectrum obtained from $Fe_3(CO)_{12}$ (Figure 4b) was markedly different from the spectra of $Ru_3(CO)_{12}$ and $Os_3(CO)_{12}$. Clustering also occurs for $Fe_3(CO)_{12}$, and clusters with much higher nuclearities, ca. 40 iron atoms, were produced. In addition, fragmentation of the cluster was evident, with strong peaks corresponding to mononuclear iron species. Interpretation of the spectrum is complicated by the fact that [Fe] and [2CO] have similar mass ([^{56}Fe] 55.935 Da and [$2^{12}C^{16}O$] 55.990 Da), and hence, with the exception of $[Fe(CO)]^-$, all assignments are somewhat ambiguous with the level of mass resolution available. The cluster peaks extend out to ca. 3500 Da, at which point they appear as "waves" or "ripples" in the baseline. A mass of 3500 Da could represent any number of large clusters, $Fe_{35}(CO)_{55}$ and $Fe_{45}(CO)_{35}$ being two possibilities.

The presence of mononuclear species suggests that, at least in part, the $Fe_3(CO)_{12}$ precursor cluster is broken up prior to, or during, the supracluster-forming process. Whether the main building blocks for supracluster formation are mono- or dinuclear fragments or the original trinuclear cluster remains unclear, and we hope to delineate this by LDI-FT-ICR mass spectrometry and by studying the growth of a series of heteronuclear clusters.

Concluding Comments

The UV-LDI mass spectra of $[Ru_3(CO)_{12}]$, $[Os_3(CO)_{12}]$, and $[Fe_3(CO)_{12}]$ have many similarities (vide infra). The differences, however, may be explained, at least in part, from the differences in metal−metal bond strengths between these three transition metals.[25] The most intense peaks in the spectrum of $[Os_3(CO)_{12}]$ correspond to the trinuclear species $[Os_3(CO)_{11}]^-$, $[Os_3(CO)_{10}]^-$, and

$[Os_3(CO)_9]^-$. Clustering takes place but not to the same extent as that observed for the iron and ruthenium analogues. The nuclearities of the most prominent osmium clusters correspond to four, five, six, and eight. No mononuclear or dinuclear fragmentation products are observed in the spectra obtained from $[Os_3(CO)_{12}]$. In contrast, the spectra obtained using $[Fe_3(CO)_{12}]$ as precursor show extensive fragmentation and aggregation products compared with the other two cluster precursors. It is difficult to give precise assignments for the iron clusters observed since iron has the same nominal mass as two CO ligands. The clustering exhibited by $[Ru_3(CO)_{12}]$ is intermediate between that observed for the osmium and iron precursors, although it is more like that of osmium. These observations are in keeping with the general chemical trends expected for the group 8 carbonyls.

Experimental Section

The cluster $[Ru_3(CO)_{12}]$ was prepared according to the literature method.[26] The clusters $[Fe_3(CO)_{12}]$ and $[Os_3(CO)_{12}]$ were purchased from Aldrich and used as supplied. These precursors were dissolved in dichloromethane and deposited onto the sample probe. The solvent was allowed to evaporate, leaving a thin layer of the pure sample. Several layers were added in this manner.

An examination of the effect of changing the sample morphology was carried out. Single crystals, powdered samples, and the effect of changing the solvent used to layer the sample as well as the number of layers were all examined. Qualitatively the spectra were similar regardless of how the sample was prepared. Therefore, the solvent evaporation method was employed in subsequent experiments since it was the simplest to carry out. Spectra were recorded using a Micromass TOFSpec-SE instrument for $[Ru_3(CO)_{12}]$ and a Micromass TOFSpec-2E instrument for $[Os_3(CO)_{12}]$ and $[Fe_3(CO)_{12}]$. Calibration was carried out before each new sample using PEG standards, and the instrumental parameters were standard settings.[27] Qualitatively identical spectra were obtained using a Kratos KOMPACT 4 MALDI-TOF instrument.

Acknowledgment. We would like to thank the Royal Society for a University Research Fellowship (P.J.D.) and the New Zealand Foundation for Research, Science and Technology for a Postdoctoral Fellowship (J.S.M., Contract CAM801). We would also like to thank Dr. John E. McGrady (University of York) for helpful discussions concerning the work described herein.

OM990075F

(25) Housecroft, C. E.; Wade, K.; Smith, B. C. *J. Chem. Soc., Chem. Commun.* **1978**, 765.

(26) Johnson, B. F. G.; Lewis, J.; Kilty, P. A. *J. Chem. Soc. A* **1968**, 2859.

(27) Bateman, R. H.; Brown, J. M.; Critchley, W. G.; Cambell, S.; Williams, T.; Scrivens, J. H.; Jackson, A. T. Technical Note 104, Micromass, 1997.